AIP | Review of Scientific Instruments

Ion Focusing Properties of a Quadrupole Lens Pair

H. A. Enge

Citation: Review of Scientific Instruments **30**, 248 (1959); doi: 10.1063/1.1716528
View online: http://dx.doi.org/10.1063/1.1716528
View Table of Contents: http://scitation.aip.org/content/aip/journal/rsi/30/4?ver=pdfcov
Published by the AIP Publishing

TE_{211} modes, and from these measurements a graph was plotted of the fractional change in length as a function of temperature (see Fig. 2). From this graph and the measurements of the TE_{011} mode for the combined barium titanate and brass cavity, the diameter of the barium titanate cylinder was calculated for various temperatures (see Fig. 3). The discontinuities which occur in the slope of the graph correspond to phase transitions[3] from tetragonal to orthorhombic (5°C) and from orthorhombic to rhombohedral (−80°C). At each of the transitions, the deformation of a single crystal of barium titanate is such as to produce expansion along the direction of spontaneous polarization.

[3] E. T. Jaynes, *Ferroelectricity* (Princeton University Press, Princeton, New Jersey, 1953), p. 19.

As a check on the validity of the above procedure, a copper cylinder of similar dimensions was used in place of the barium titanate, and the coefficient of thermal expansion of the copper measured. The results obtained in this manner were compared with those obtained by Nix and MacNair.[4] The comparison showed good agreement (see Fig. 4).

ACKNOWLEDGMENTS

The authors wish to express their thanks to the National Research Council, the Defense Research Board, and Dalhousie University, Nova Scotia, for the provision of grants and facilities which made this work possible.

[4] F. C. Nix and D. MacNair, Phys. Rev. **60**, 597 (1941).

THE REVIEW OF SCIENTIFIC INSTRUMENTS VOLUME 30, NUMBER 4 APRIL, 1959

Ion Focusing Properties of a Quadrupole Lens Pair*

H. A. ENGE

Department of Physics and Laboratory for Nuclear Science, Massachusetts Institute of Technology, Cambridge 39, Massachusetts

(Received December 24, 1958; and in final form, January 19, 1959)

The focusing properties of a quadrupole lens pair have been studied, and the results of thick-lens calculations are presented in the form of graphs showing the field strength parameters and magnifications as functions of object and image distances.

1. INTRODUCTION

SINCE the invention of the strong-focusing principle for ion optics,[1,2] a number of papers have been written[3–9] describing theoretical or practical aspects of quadrupole lens pairs. A presentation of the results of calculations on focusing properties in a form convenient to use in practice seems to be lacking in the literature. This paper is intended to fill this gap.

2. CALCULATIONS OF FOCAL STRENGTHS

Figure 1 shows the particle trajectories in two planes of a quadrupole lens pair. In the case shown, the object and image distances are the same in both planes. The following graphical procedure of solving the equations for the focal strengths of the two lenses can be used also when astigmatic focusing is wanted.

The x-y plane is referred to as the diverging plane (last lens diverging). In this plane, the magnification in a symmetric case ($a=b$) is greater than unity. In the x-z plane, the converging plane, the magnification is smaller than unity for a symmetric case.

In the converging plane, the particle trajectories can be expressed as[10]

$$\begin{aligned}&\text{First lens,}\quad z=Z_1\cosh[k_1(x-a)+\phi_1] \quad \text{for} \quad k_1a>1\\ &\qquad\qquad z=Z_1\sinh[k_1(x-a)+\phi_1'] \quad \text{for} \quad k_1a<1, \quad (1)\\ &\text{Second lens } z=Z_2\cos[k_2(x-x_{III})+\phi_2],\end{aligned}$$

where $x_{III}=a+s+2l$.

The reason why one function cannot describe the trajectories in the first lens for all possible cases will be apparent later [Eq. (3)].

The field parameters, or wave numbers k_1 and k_2, are given by the relationships

$$\begin{aligned}k&=\frac{1}{d}\left(\frac{3.2\pi IN}{B\rho}\right)^{\frac{1}{2}}\ \text{cm}^{-1} \quad \text{magnetic lens,}\\ k&=\frac{2}{d}\left(\frac{nV}{E}\right)^{\frac{1}{2}}\ \text{cm}^{-1} \quad \text{electrostatic lens,}\end{aligned} \quad (2)$$

* This work has been supported in part through U. S. Atomic Energy Commission Contract AT(30-1)-2098 with funds provided by the U. S. Atomic Energy Commission, by the Office of Naval Research, and by the Air Force Office of Scientific Research.

[1] N. C. Christofilos, U. S. Patent No. 2,736,799.

[2] Courant, Livingston, and Snyder, Phys. Rev. **88**, 1190 (1952).

[3] A. Vash, M. S. thesis, Massachusetts Institute of Technology, 1953 (unpublished).

[4] Shull, MacFarland, and Bretscher, Rev. Sci. Instr. **25**, 364 (1954).

[5] W. C. Elmore and M. W. Garrett, Rev. Sci. Instr. **25**, 480 (1954).

[6] Dayton, Shoemaker, and Mozley, Rev. Sci. Instr. **25**, 485 (1954).

[7] Struński, Cooper, Frisch, and Zimmerman, Rev. Sci. Instr. **25**, 514 (1954).

[8] M. L. Bullock, Am. J. Phys. **23**, 264 (1955).

[9] D. A. Bromley and J. A. Bruner, University of Rochester Report No. NYO-3823.

[10] H. A. Enge, Rev. Sci. Instr. **29**, 885 (1958).

where d is the aperture diameter of the lens in centimeters (pole tip to pole tip). In the magnetic case, $B\rho$ is the magnetic rigidity of the particles in gauss centimeters, and IN is the number of ampere turns *per pole* available for driving the flux through the air gap. In the electrostatic case, V is the potential on the poles in volts (+ and −), and n is the number of elementary charges carried by the particle. In a nonrelativistic case, E is the kinetic energy of the particle in electron volts. In general, it is $E=p\beta c/2$ (in electron volts).

Boundary conditions at I and III will give (still with reference to the converging plane only)

$$\text{I:}\begin{cases}\tanh\phi_1=\dfrac{1}{k_1a} & \text{for } k_1a>1\\ \coth\phi_1'=\dfrac{1}{k_1a} & \text{for } k_1a<1\end{cases}\qquad(3)$$

$$\text{III: } \tan\phi_2=\frac{1}{k_2b}.$$

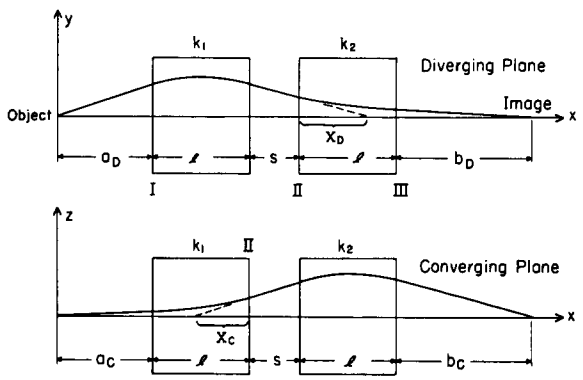

FIG. 1. Particle trajectories in two planes of a quadrupole lens pair.

The fact that the tangent to the hyperbolic curve at the exit of the first lens must cross the x axis at the same point as the tangent to the trigonometric curve from the entrance of the second lens can be used as a boundary condition at II ($X_C=X_C$, see Fig. 1). This requirement leads to the following relationship:

$$\begin{aligned}&\frac{1}{k_1l}\coth[k_1l+\phi_1]=\frac{1}{k_2l}\cot[k_2l-\phi_2]-\frac{s}{l} && \text{for } k_1a>1,\\ &\frac{1}{k_1l}\tanh[k_1l+\phi_1']=\frac{1}{k_2l}\cot[k_2l-\phi_2]-\frac{s}{l} && \text{for } k_1a<1.\end{aligned}\qquad(4)$$

Since ϕ_1 or ϕ_1' and ϕ_2 are simple functions of k_1 and k_2 [Eq. (3)], Eq. (4) gives one relationship between k_1 and k_2. Another equation is obtained, of course, by considering the focusing conditions in the diverging plane. In the case that stigmatic focusing is desired, one obtains the second

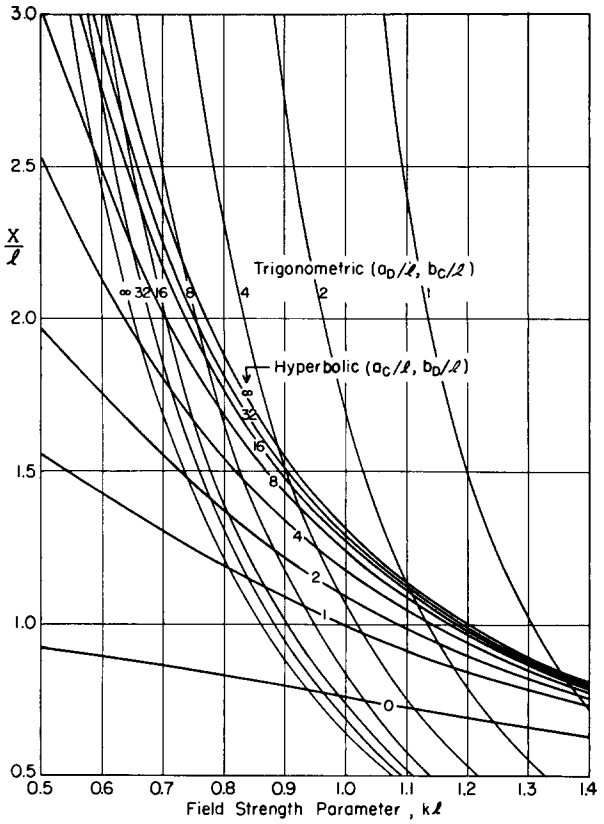

FIG. 2. Graph used for determining the field strength parameters (wave numbers) k_1 and k_2.

equation simply by substituting a for b, k_1 for k_2, and vice versa in Eq. (4).

In Fig. 2, the set of curves marked "hyperbolic" represents the left-hand side of Eq. (4). The curves have been plotted *versus* kl with the relative object distance in the converging plane a_C/l and the relative image distance in the diverging plane b_D/l as parameters. The set of curves marked "trigonometric" represents the right-hand side of Eq. (4) with $s/l=0$.

The procedure followed in determining k_1 and k_2 is demonstrated in Fig. 3, which shows sections of Fig. 2. In Fig. 3(a) is shown the solution for a stigmatic case with $a=2l$ and $b=4l$. In Fig. 3(b) is shown the solution in a case where $b=2l$, $a_D=l$, and $a_C=4l$ (astigmatic

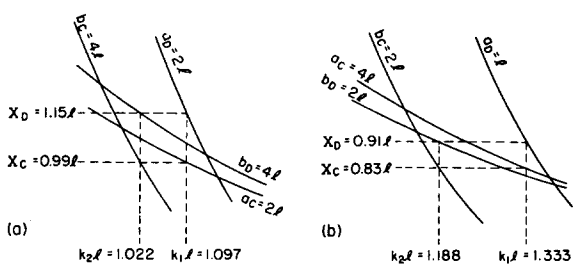

FIG. 3. Examples of wave-number determinations (a) for a stigmatic case, $a=2l$; $b=4l$; (b) for an astigmatic case, $a_D=l$; $a_C=4l$; $b=2l$. For both examples, $s=0$.

object). In addition to the field strength parameters $k_1 l$ and $k_2 l$, the solution gives the values of X_D and X_C. These are of no further importance, however.

In the case that the lens separation s/l is not equal to zero, the procedure is exactly the same, except that the trigonometric curves are shifted down in Fig. 2 by the amount s/l [see Eq. (4)].

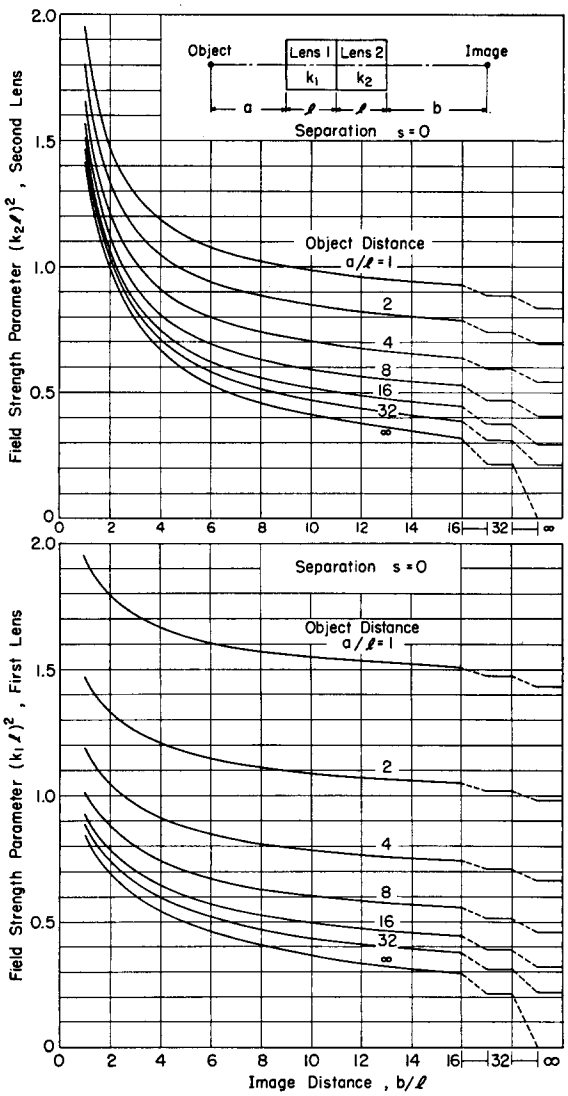

FIG. 4. Field strength parameters [defined by Eq. (2)] *vs* object and image distances for zero lens separation, $s=0$.

Figures 4 and 5 give results of the calculations of k_1 and k_2 for various object and image distances and for two stigmatic cases with $s/l=0$ and $s/l=1$. The results are presented as the value of $(kl)^2$, a nondimensional quantity that is proportional to the pole potential [ampere-turns or voltage, see Eq. (2)]. It is clear from a comparison between the two figures that an increase in the lens distance s results in a reduction in the lens strengths needed

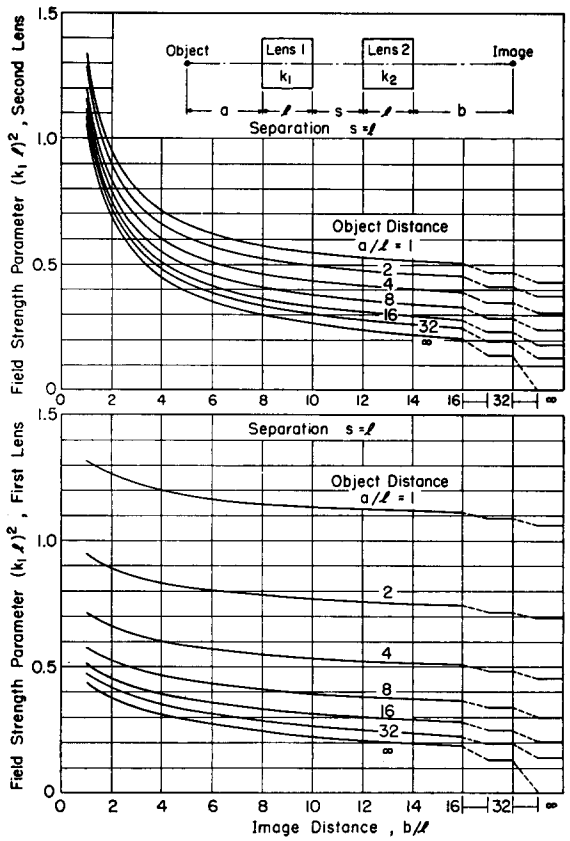

FIG. 5. Field strength parameters [defined by Eq. (2)] *vs* object and image distances for lens separation, $s=l$.

when a and b are kept constant. If, however, $a+s/2$ and $b+s/2$ are kept constant (giving a constant object-to-image distance), the situation is somewhat different. There exist then optimum values of s/l, for which k_1 and k_2 reach minima.

III. MAGNIFICATION

Simple expressions for the magnification of the lens system can be found for instance by considering the particle trajectory that, between the two lenses, is parallel

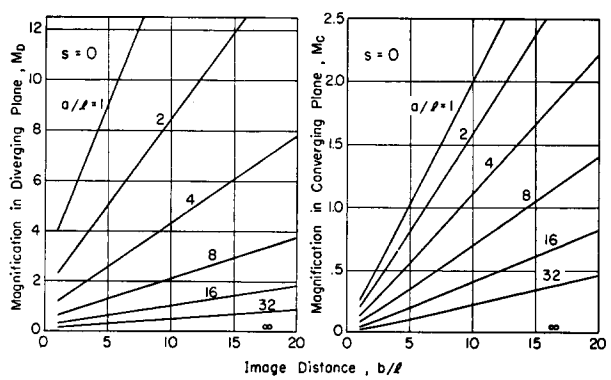

FIG. 6. Magnification factors *vs* object and image distances for lens separation, $s=0$.

to the axis. The result is for the converging plane

$$M_C=\frac{bk_2\sinh k_2l-\cos k_2l}{ak_1\sinh k_1l+\cosh k_1l}, \tag{5}$$

and for the diverging plane

$$M_D=\frac{bk_2\sinh k_2l+\cosh k_2l}{ak_1\sinh k_1l-\cos k_1l}. \tag{6}$$

In Figs. 6 and 7 are plotted the results of calculations of magnification factors for various object and image distances and for two values of the lens separation, $s=0$ and $s=l$.

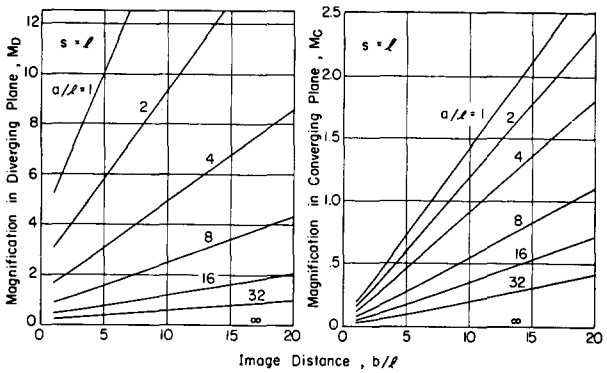

FIG. 7. Magnification factors *vs* object and image distances for lens separation, $s=l$.

IV. FINAL REMARKS

The actual length of the lenses will be in excess of the length of the pole pieces, because of the fringing field at both ends. If the two lenses are as close to each other ($s\approx 0$) as they can be without causing saturation difficulties in the magnetic case and short circuit in the electric case, the range of the fringing field between the two lenses will necessarily be short. At the free ends, it is probably also wise to cut down on the range of the fringing field by shielding (magnetic or electrostatic as the case may be). In the calculations above, the lens length should be taken as

$$l=l_{pp}+fd,$$

where l_{pp} is the length of the pole pieces, d is the aperture diameter, and f is a factor that depends upon the design. It is unlikely that it will ever be larger than unity.

THE REVIEW OF SCIENTIFIC INSTRUMENTS VOLUME 30, NUMBER 4 APRIL, 1959

Recording Optical Pyrometer*

NORMAN A. BLUM
Avco Manufacturing Corporation, Research and Advanced Development Division, Wilmington, Massachusetts
(Received December 8, 1958; and in final form, January 6, 1959)

A recording pyrometer which measures the brightness temperature at 0.65 μ of a small incandescent sample in the range 1300°C to above 3000°C with a time constant of a few milliseconds is described. The instrument, designed to be used in studies of materials exposed to the plasma jet of a high-intensity electric arc, is reliable to within ±20°C, and is suitable for measuring transient high-temperature fluctuations or for applications where use of a standard optical pyrometer might be hazardous to personnel.

INTRODUCTION

EXPERIMENTAL work with small samples of material exposed to the plasma jet of a high-intensity electric arc calls for a means of measuring the temperature of such samples. The plasma jet[1,2] may be operated at a temperature as high as 10 000°K, and heat transfer rates as great as 2×10^7 Btu/ft^{2}hr at various flow velocities and pressures may be obtained. A sample exposed to such intense heat flux rapidly becomes incandescent and is usually destroyed within seconds. The disappearing filament type optical pyrometer, which has been used at this laboratory in the past, has proved unsatisfactory in two respects: (a) the reaction time of the operator is too slow to obtain consistent temperature readings during the few seconds of arc operation; and (b) the operator must be in the vicinity of the dangerously hot arc.

An instrument is desired which operates unattended during the period the arc is operating and which gives a recorded history of the sample surface temperature with a reliability somewhat better than that of the optical pyrometer. Under the conditions which prevail during operation of the arc, it is difficult to obtain temperature readings with the optical pyrometer which may be considered reliable to within 100°C; it is also difficult to obtain more than one measurement during the interval the arc is in operation.

The standard optical pyrometer is calibrated to measure

* Work done under U. S. Air Force Contract AF-04(645)-30.
[1] G. M. Giannini, Sci. American **197**, 80 (August, 1957).
[2] W. Finkelnburg and H. Maecker, in *Handbuch der Physik*, (Springer-Verlag, Berlin, 1956), Vol. XXII, pp. 224–444.